HHS Public Access

Author manuscript

Am J Ophthalmol. Author manuscript; available in PMC 2016 April 01.

Published in final edited form as:

Am J Ophthalmol. 2015 April ; 159(4): 803–811. doi:10.1016/j.ajo.2015.01.017.

Assessment of Retinal Nerve Fiber Layer Thickness in Healthy, Full-Term Neonates

Adam L. Rothman[1], **Monica B. Sevilla**[1], **Sharon F. Freedman**[1,2], **Amy Y. Tong**[1], **Vincent Tai**[1], **Du Tran-Viet**[1], **Sina Farsiu**[3,1], **Cynthia A. Toth**[1,3], and **Mays A. El-Dairi**[1,2]

[1]Department of Ophthalmology, Duke University Eye Center, Erwin Rd, Durham, NC, 27710, USA

[2]Department of Pediatrics, Duke University School of Medicine, Durham, NC, 27710, USA

[3]Department of Biomedical Engineering, Duke University, Durham, NC, 27708, USA

Introduction

The retinal nerve fiber layer (RNFL) consists of ganglion cell axons that course as the inner surface of the neurosensory retina and, after converging as the optic nerve, extend to the lateral geniculate nucleus of the brain. Spectral-domain optical coherence tomography (SDOCT) imaging provides in vivo visualization of this central nervous system (CNS) tract and allows quantification of ganglion cell axonal loss by segmentation. Peripapillary RNFL measurements were originally used to assess optic nerve axonal integrity in glaucomatous versus normal adults' eyes[1,2] and later adapted to monitor other optic neuropathies.[3] Similarly, measuring RNFL thicknesses in children improves diagnosis and monitoring of optic neuropathies unique to the pediatric population[4–11] and can identify differences in CNS tissue between children with a history of preterm versus full-term birth.[12–15] While normative data of RNFL thicknesses exists for school-age children,[11,16–24] this data is lacking during the neonatal period (PubMed Mesh search terms, nerve fiber layer AND infant), while the immature optic nerves are still growing and undergoing myelination.[25–27]

Portable hand-held SDOCT allows for bedside cross-sectional assessment of the retina and optic nerve in non-traditional environments including the nursery.[28–31] Our understanding of perinatal eye development and maturation has improved by comparing posterior segment microanatomy observed on SDOCT in preterm infants to that of full-term infants imaged in the nursery and further relating microanatomic abnormalities to ophthalmologic and

Corresponding Author: Mays A. El-Dairi, MD, Department of Ophthalmology, Duke University Medical Center, 2351 Erwin Road, Durham, NC 27710, Phone: 919-684-9191, Fax: 919-681-0547, mays.el-dairi@dm.duke.edu.

Its contents are solely the responsibility of the authors and do not necessarily represent the official view of NCRR, NEI, or NIH.

Author Contributions: Design of the study (AR, MS, SFF, AT, SF, CT, ME); Conduct of the study (AR, MS, SFF, AT, VT, DT, CT, ME); Collection of data (AR, MS, SFF, AT, VT, DT, SF, CT, ME); Management of data (AR, MS, CT, ME); Analysis of data (AR, MS, SFF, CT, ME); Interpretation of data (AR, MS, SFF, VT, DT, CT, ME); Preparation of manuscript (AR, MS, SFF, VT, CT, ME); Review of manuscript (AR, MS, SFF, AT, VT, DT, SF, CT, ME); Approval of manuscript (AR, MS, SFF, AT, VT, DT, SF, CT, ME)

Financial Disclosures: Dr. Toth receives royalties through her university from Alcon and research support from Bioptigen and Genentech. She and Dr. Farsiu also have unlicensed patents pending in OCT imaging and analysis. No other authors have financial disclosures. No authors have a proprietary interest in the current study.

systemic pathology.[32–40] In particular, analysis of SDOCT images allows for reproducible quantification of optic nerve head parameters as an estimate of ganglion cell axonal integrity in both full-term[32] and age-matched preterm infants.[33] Retinal nerve fiver layer thickness has previously been measured in young children with optic pathway gliomas while they were sedated for magnetic resonance imaging using a hand-held SDOCT system[5,41] and demonstrated to be reproducible.[9,41–43] The present study's purpose was to reproducibly quantify RNFL thickness in full-term neonates and thereby to provide normative data for future analyses.

Methods

The current analysis is part of a larger, prospective study of retinal and optic nerve development that was approved by the Duke University institutional review board and adheres to the Health Insurance Portability and Accountability Act and all tenets of the Declaration of Helsinki. All infants were enrolled and imaged from August 2010 through May 2011 with parent or legal guardian written informed consent. Infants were eligible if born at or after 37 weeks post-menstrual age (PMA) and before 43 weeks PMA with no known medical conditions and deemed clinically stable by the pediatric care team to undergo SDOCT imaging. All infants were imaged following clinical examination, which included dilated fundus examination using indirect ophthalmoscopy. Spectral domain optical coherence tomography imaging was performed according to an age-specific protocol described by Maldonado et al[29] and Cabrera et al.[44] using a portable, handheld SDOCT system (either an early research system or the Envisu 2200, Bioptigen, Inc., Research Triangle Park, NC) approaching the eyes over the forehead of the supine infant. Demographic information was collected from medical records, including gestational age, birth weight, gender and parent-reported race.

One eye per infant was randomly selected for inclusion in the study; the fellow eye was considered for analysis if the primary eye did not have an adequate SDOCT scan for RNFL analysis. The best vertical SDOCT volume scan that contained the optic disc and macula was selected for each infant. Criteria considered when selecting the best scan included: focus, alignment, tilt, and the ability to differentiate retinal layers. Scans were excluded if there was eye movement that caused skipping or lags between B-scans, inadequate visualization of the center of the optic disc, or if the axis between the center of the optic nerve and fovea could not be determined. All SDOCT scans were converted to tagged image file format, and were registered with ImageJ v 1.43r (National Institute of Health, Bethesda, MD).

Several custom MATLAB scripts (Mathworks, Inc., Natick, MA) were utilized for quantitative analysis. Graders were masked to all demographic information other than age at imaging. The SDOCT images were captured using a handheld device on neonates in the supine position who could not fixate on a central target. Thus, the organizing axis from the foveal center to the optic nerve head determined the direction of the image frame. This is an adaptation of the method described by He et al[45] and Chauhan and Burgoyne[46] for measurements of the optic nerve and peripapillary structures in adults. Two certified pediatric SDOCT graders (A.L.R. and D. T.-V.) used Duke OCT Retinal Analysis Program

(DOCTRAP) v 60.2, an automatic segmentation program based on graph theory and dynamic programming,[47] to mark the center of the optic disc as well as the fovea on each infant's pertinent B-scan; if the fovea was not visualized, the midpoint between the superior and inferior arcades was marked as the axis of the fovea. Graders determined the center of the optic disc by centering a 2 mm radius annulus on the optic disc using DOCTRAP. A MATLAB script read the marked coordinates of the center of the optic disc and fovea and created an organizing axis between the two for each volume. After DOCTRAP segmented the superior and inferior borders of the RNFL for each volume, graders manually corrected any segmentation requiring adjustment (Figure 1, left). The two segmentation lines were set at the same height for any portion of a B-scan that was of too poor quality for segmentation in order to measure a thickness of zero.

The graphic user interface could then measure the average RNFL thickness at an arc of any set distance from the optic nerve to the fovea (Figure 2). The program considered only RNFL thicknesses greater than 5 microns, allowing portions of the arc that were unable to be segmented to be excluded from the average thickness calculations. The arc only measured the retina temporal to the optic nerve; nasal retina was not imaged as it is technically more difficult to image and more time consuming on a non-sedated full-term newborn. This arc could then be divided into sectors to provide regional average RNFL thicknesses. The temporal macula was divided into four 45° arcs, considered from superior to inferior, the superior temporal, temporal superior, temporal inferior, and inferior temporal sectors (Figure 1, middle). The temporal superior and temporal inferior arcs were also assessed together as the 90° temporal quadrant. The user could set a minimum threshold of percent of the arc adequately segmented in order for each quadrant's thickness to be calculated if this data availability threshold was met. The minimum threshold for the current analysis was chosen as 90% segmentation. For example, 90% of an eye's superior temporal sector must be segmented in order to calculate the average RNFL thickness within this sector; infants who have a thickness of 5 microns or less for 11% or more of this sector would not be included in the analysis. In addition, the average RNFL thickness was calculated for the papillomacular bundle (PMB), defined as the 30° arc from −15° to +15° on the axis from the optic nerve to fovea (Figure 2) and also referred to as the 9 o'clock hour for right eyes and 3 o'clock hour for left eyes.

Adult RNFL analyses typically measure average RNFL thicknesses at a radius of 1.70–1.75 mm from the center of the optic nerve.[48] Because the infant eye is still growing and has a smaller distance from the center of the optic nerve to the fovea,[49] the optimal distance for RNFL measurements in neonates is unknown. The average RNFL thickness at the PMB for each infant was calculated at arcs with radii of 1.1, 1.3, 1.5, and 1.7 mm from the center of the optic disc (Figure 1, right). The distributions of these RNFL thicknesses for all infants at each arc distance were assessed for normality to determine the optimal distance for subsequent analyses. The mean RNFL thickness at 1.7 mm from the optic nerve center for each geographic sector was also computed to allow comparisons to the pediatric literature.

Once this distance was determined, the average RNFL thickness along the PMB arc was compared by sex, race, and eye side as well as analyzed by gestational age and birth weight. The average RNFL within the superior temporal, temporal superior, temporal inferior,

inferior temporal sectors as well as the temporal quadrant were then compared by race. Any infants that were part of a previous study that measured optic nerve parameters observed on SDOCT had their optic nerve vertical cup-to-disc ratio compared to their average RNFL thickness measurement.[33]

Intrauser, interuser, and intravisit reproducibility of average PMB thickness were assessed to validate this novel method of neonatal RNFL thickness measurement. Intrauser and intravisit reproducibility were performed by one user (A.L.R.) while interuser reproducibility was assessed between both users (A.L.R. and D. T.-V.). All reproducibility segmentation correction and marking of the fovea and optic nerve center was performed while masked to the prior reading. Intrauser and interuser reproducibility of average RNFL thickness at the PMB considered 20 randomly selected infants. All infants who had two separate scans in the same eye of adequate quality for analysis obtained from the same imaging session were considered for intravisit reproducibility. All reproducibility scans had optic nerves and foveae remarked and were resegmented with new segmentation correction performed.

Statistical analysis was performed using JMP Pro v 11 (SAS Institute Inc., Cary, NC). P-values were considered statistically significant if less than 0.05. Normality of average RNFL distributions in the full-term cohort was assessed by Shapiro-Wilk W tests where a $P<0.05$ rejects the null hypothesis that the distribution is normal. The difference in mean RNFL thickness at the PMB at different distances from the optic nerve center was assessed with an analysis of variance test. The relationships between average RNFL thickness along the PMB arc and sex were assessed by a two-tailed t-test while average RNFL thickness along the PMB arc was compared between races by a Kruskal-Wallis test. The average RNFL within the superior temporal, temporal superior, temporal inferior, inferior temporal sectors as well as the temporal quadrant were compared by race with the Kruskal-Wallis test and then between racial groups by the Tukey-Kramer method. Bonferroni correction for comparisons of RNFL thickness by fundus sector between races required a P-value less than 0.01 to demonstrate statistical significance. Additionally, the relationship between average RNFL thickness along the PMB arc and GA and birth weight were assessed by linear regression. The relationship between optic nerve vertical cup diameter, vertical disc diameter, and vertical cup-to-disc and average RNFL thickness along the PMB arc was assessed by linear regression using previously described full-term optic nerve parameters.[32] Intrauser, interuser, and intravisit reproducibility of average RNFL thickness at the PMB were summarized by the intraclass correlation coefficient (ICC).

Results

Demographics

A total of 57 full-term infants were enrolled in the study with one infant withdrawn prior to SDOCT imaging. Of the 56 full-term infants who underwent SDOCT imaging, 50 full-term infants had at least one adequate SDOCT for RNFL analysis. A total of 45 of the full-term infants included in the current study had their optic nerve parameters, but not their RNFL, measured in a previous report.[33] The mean ± standard deviation (SD) gestational age and birth weight of all infants was 39.2 ± 1.1 weeks PMA and 3356 ± 458 g, respectively. The

cohort included 22 (44%) males. There were 12 (24%) Black, 20 (40%) Hispanic, and 18 (36%) White full-term infants.

Distance from Optic Nerve for Retinal Nerve Fiber Layer Measurements

All 50 full-term infants had 100% of their RNFL segmented at a distance of 1.5 and 1.7 mm from the center of the optic nerve; while two infants did not have at least 90% of their respective RNFL segmented at the PMB, one with inadequate segmentation at a distance of 1.1 mm and the other at 1.3 mm from the center of the optic nerve, the remaining 49 infants had 100% of their RNFLs measured at these arc distances. The mean ± SD average (P-value for Shapiro-Wilk W test of normality) RNFL thicknesses for all full-term infants assessed at 1.1, 1.3, 1.5, and 1.7 mm distances from the center of the optic nerve at the PMB were 88 ± 17 μm (P=0.11), 80 ± 17 μm (P=0.22), 72 ± 13 μm (P=0.60), and 64 ± 12 μm (P=0.34), respectively (Figure 3). The mean RNFL at the PMB decreased significantly when measured further away from the optic nerve (P<0.001). All subsequent analyses involve thicknesses measured along the PMB arc at a distance of 1.5 mm from the center of the optic nerve because this distance had the most normally distributed average RNFL thicknesses and the literature suggests that a distance of 1.5 mm from the center of the optic nerve in newborns is proportional to the 1.7 mm distance considered for adults.[48–50]

Average Sectoral Retinal Nerve Fiber Layer Thicknesses

The mean ± SD average RNFL thicknesses for all full-term infants assessed at a distance of 1.5 mm from the optic nerve center along the PMB, superior temporal, temporal superior, temporal inferior, inferior temporal, and temporal sectors were 72 ± 13 μm, 117 ± 28 μm, 81 ± 20 μm, 85 ± 20 μm, 118 ± 29 μm, and 83 ± 16 μm, respectively. There was no significant difference in average RNFL thickness along the PMB arc at 1.5 mm from the center of the optic nerve between males (69 ± 14 μm) and females (73 ± 13 μm, P=0.31) or between Black (74 ± 15 μm), Hispanics (74 ± 13 μm, P=0.16), and White (67 ± 11 μm) infants. Additionally, there was no relationship between average RNFL thickness along the PMB arc at 1.5 mm distance and GA (R^2<0.01, P=0.70) or birth weight (R^2=0.01, P=0.46) in this full-term cohort. There was a trend towards greater average superior temporal RNFL thickness for Blacks (128 ± 27 μm, P=0.04) as well as Hispanics (124 ± 30 μm, P=0.04) compared to White infants (100 ± 19 μm); there was no difference in the average RNFL thicknesses for the temporal superior, temporal inferior, and inferior temporal sectors or the temporal quadrant when comparing races (Table 1). There was no relationship between average RNFL thickness along the PMB arc at a distance of 1.5 mm and optic nerve vertical cup diameter (R^2<0.01, P=0.53), vertical disc diameter (R^2=0.02, P=0.32), or vertical cup-to-disc ratio (R^2=0.04, P=0.22) in this healthy full-term cohort.

Reproducibility

Intergrader and intragrader ICC (95% confidence interval) were 0.89 (0.75–0.95) and 0.94 (0.85–0.97), respectively for average RNFL thickness measured at 1.5 mm distance from the center of the optic nerve along the PMB for 20 randomly selected SDOCT scans. Intravisit ICC (95% confidence interval) was 0.76 (0.37–0.92) for 12 infants who had two adequate SDOCT scans at the time of imaging.

Discussion

To our knowledge, this is the first report of average sectoral RNFL thickness measurements in healthy, full-term infants. We propose that neonatal RNFL thickness should be assessed at a radial distance of 1.5 mm from the center of the optic disc. There was a trend towards thicker superior temporal sector of RNFL for Black and Hispanic versus White infants; however, there were no other significant racial variations identified in this sample. We found no significant variation in average RNFL thicknesses along the PMB arc by any demographic parameters; nor did we identify any significant relationship between average sectoral RNFL thickness and optic nerve vertical cup diameter, vertical disc diameter, or vertical cup-to-disc ratio in eyes of healthy, full-term newborns. This report will hopefully provide useful data to serve as a normative dataset for future RNFL analyses during the neonatal period aimed at detecting and/or monitoring neonatal eye pathology.

Because the infant cannot cooperate to fixate for the examination, an important method in our analysis was to utilize capture of volume scans that included optic nerve and fovea. Although all imaging was captured from over the forehead of the infant, by utilizing the axis between the fovea and the center of the optic nerve as an orienting axis for all measurements, we were able to analyze images taken at slightly different rotation and without requiring fixation on a set target. This method of orientation relates to the work of He et al[45] and Chauhan and Burgoyne[46] who have demonstrated the utility of the fovea to Bruch's membrane opening axis to standardize optic nerve rim and RNFL measurements in adult patients.

Because the eye's dimensions change with growth during infancy, we suggest that the traditional distance of 1.7 mm arc radius from the center of the optic disc at which the RNFL is measured is not appropriate for neonates. Schuman et al.[48] initially evaluated the reproducibility of circumpapillary RNFL measurements in adult eyes at radii of 1.45, 1.7, and 2.25 mm from the center of the optic nerve head. They found better reproducibility at the 1.7 mm radius than the 1.45 mm radius as the smaller annulus may overlap with the optic nerve head. They also argued that the 2.25 mm radius circle would not be as sensitive as the 1.7 mm radius at detecting subtle RNFL differences because 2.25 mm is relatively distant from the optic nerve head. Thus, RNFL thickness is traditionally assessed at a distance of 1.70–1.75 mm radius from the center of the optic disc, regardless of age. However, De Silva et al.[49] measured the distance from the center of the optic nerve and fovea in 51 infants at 32 to 50 weeks PMA using digital fundus photography and found a mean distance of 4.4 mm. Williams and Wilkinson[50] measured a mean distance of 4.9 mm between these two anatomic landmarks in adults. These studies suggest the proportional age-adjusted annulus distance to measure RNFL thicknesses is a 1.53 mm radius from the optic disc center. Furthermore, as shown previously on histology study of postmortem adult eyes, we found that the RNFL in newborns is significantly thicker when measured closer to the optic nerve.[51] The current study further validates 1.5 mm as the appropriate radius as it had a more normal distribution than the average RNFL thicknesses measured along the PMB at distances of 1.1, 1.3, and 1.7 mm from the center of the optic nerve in our healthy newborn cohort.

Previous studies of optic nerve development suggest large changes in posterior segment neural tissue both during gestation and early life. The RNFL is the anterior manifestation of the optic nerve axons within the neurosensory retina and its thickness may vary according to the degree of nerve maturation and myelination. Provis et al.[25] observed a peak of 3.7 million axons in the optic nerve at 16–17 weeks PMA and noted this count decreases by approximately 70% prior to term birth. While approximately 75% of optic nerve growth occurs in utero, the optic nerves are largely unmyelinated at birth, with complete myelination occurring by 2 years of age.[26,27] The optics of the eye rapidly change over this time window. In particular, the axial length, which increases approximately 7 mm from infancy through adulthood,[52] can influence measured RNFL thicknesses.[53,54] Thus, the neonatal RNFL has unique characteristics that may be properly described only by its own normative dataset.

Several studies have utilized SDOCT to analyze both optic nerve parameters and RNFL measurements by race in the pediatric population. Allingham et al.[32] reported a trend toward smaller cup-to-disc ratio in White full-term infants vs. Black (P=0.07) but not Hispanic infants (P=0.29). Tong et al.[33] found that, when considering only full-term infants, the vertical disc diameter was smaller for White than Black (P=0.02) and Hispanic infants (P=0.001). They also noted, when considering both preterm and term infants, a difference in cup depth (P=0.01) among races. Although the cup-to-disc ratio is reported as larger for Black infants,[32] the temporal RNFL was generally comparable by race in the current study, possibly because the entire superior and inferior quadrants could not be measured in this study.

Comparisons to previously published pediatric normative data are only appropriate for reports that similarly examined temporal retina with the caveat that they were measured on older children at 1.7 mm from the center of the optic nerve head (Table 2). Nearly all the previous studies report temporal quadrant RNFL thicknesses that are thinner than the current study at 1.5 mm and comparable at 1.7 mm distance from the optic nerve center. Superior temporal and inferior temporal appear thinner in the current study, regardless of the radial distance from the optic nerve center. The general trend towards greater RNFL thickness in this study compared to the pediatric literature may be explained by changes in the eye optics or true change in the thickness of the RNFL that occurs with ocular growth. Additional longitudinal data would be helpful to further elucidate the mechanism of possible changes in RNFL thickness over time.

The current study, which found a trend towards thicker RNFL for Black and Hispanic infants than for White infants in the superior temporal sector but no difference in PMB or temporal RNFL thicknesses by race, is consistent with the OCT-measured RNFL literature in older children. For example, El-Dairi et al.[18] measured RNFL thickness with the OCT-3 (Carl Zeiss Meditec, Dublin, CA) in 286 children aged 3–17 years old and examined RNFL thicknesses by race and quadrants. They found the superior quadrant and total average RNFL thickness greater for both all Black versus White children (P<0.001 for both) as well as within the subset of the 64 youngest children in their study, imaged at ages 3–6 years old (P=0.001 for the superior quadrant and P=0.01 for total average RNFL). As in the current study, they also reported no racial differences in the average temporal RNFL thicknesses.

Our findings should be considered in light of several limitations. Because of the relatively small overall sample size, there were very few infants within each respective racial group. While all scans with noticeable jumps or lags were excluded, there may have been minor inconsistencies in scan acquisition that were unnoticed by graders and misrepresent the distance from the optic disc for some RNFL measurements. There may be variability related to scan tilt or blood vessel-related distortion of RNFL thickness measurements. The organizing axis for RNFL measurements was estimated based on the retinal arcades if the fovea was not visualized on the scan. Additionally, lateral measurements taken across each B-scan rely on an age-adjusted axial length model described by Maldonado et al.[29] Furthermore only the temporal retina was evaluated since the scans were captured to optimize visualization of the macula, and nasal imaging of the retina is technically difficult and time consuming in a non-sedated neonate. Thus literature comparison of current RNFL thickness measurements are only appropriate for this temporal quadrant.

We have reproducibly extracted the average temporal sectoral RNFL thickness measurements of healthy, full-term infants from SDOCT scans obtained in the first days after birth. This dataset may serve as normative information when assessing average RNFL thickness in premature infants as well as young children with pathology that causes optic atrophy such as primary congenital glaucoma or optic pathway gliomas and other tumors.

Acknowledgments

Funding/Support: The following sponsors or funding organizations who provided financial support had no role in the design or conduct of this research: The Hartwell Foundation (Toth); The Andrew Family Charitable Foundation (Toth); Research to Prevent Blindness (Toth); The Retinal Research Foundation (Toth); Grant Number 1UL1RR024128-01 from the National Center for Research Resources (NCRR), a component of the National Institutes of Health (NIH), and NIH Roadmap for Medical Research, and Grant Number P30 EY001583 from the National Eye Institute (NEI).

The authors would like to thank Sandra Stinnett of Duke University School of Medicine for assistance with statistical analysis.

References

1. Schuman JS, Hee MR, Puliafito CA, et al. Quantification of nerve fiber layer thickness in normal and glaucomatous eyes using optical coherence tomography. Arch Ophthalmol. 1995; 113:586–596. [PubMed: 7748128]
2. Savini G, Carbonelli M, Barboni P. Spectral-domain optical coherence tomography for the diagnosis and follow-up of glaucoma. Curr Opin Ophthalmol. 2011; 22:115–123. [PubMed: 21307774]
3. Pasol J. Neuro-ophthalmic disease and optical coherence tomography: glaucoma look-alikes. Curr Opin Ophthalmol. 2011; 22:124–132. [PubMed: 21307679]
4. Ely AL, El-Dairi MA, Freedman SF. Cupping Reversal in Pediatric Glaucoma-Evaluation of the Retinal Nerve Fiber Layer and Visual Field. Am J Ophthalmol. 201410.1016/j.ajo.2014.07.030
5. Avery RA, Hwang EI, Ishikawa H, et al. Handheld optical coherence tomography during sedation in young children with optic pathway gliomas. JAMA Ophthalmol. 2014; 132:265–271. [PubMed: 24435762]
6. Chang L, El-Dairi MA, Frempong TA, et al. Optical coherence tomography in the evaluation of neurofibromatosis type-1 subjects with optic pathway gliomas. J AAPOS. 2010; 14:511–517. [PubMed: 21168074]
7. El-Dairi MA, Holgado S, Asrani SG, Enyedi LB, Freedman SF. Correlation between optical coherence tomography and glaucomatous optic nerve head damage in children. Brit J Ophthalmol. 2009; 93:1325–1330. [PubMed: 19028739]

8. El-Dairi MA, Holgado S, O'Donnell T, Buckley EG, Asrani S, Freedman SF. Optical coherence tomography as a tool for monitoring pediatric pseudotumor cerebri. J AAPOS. 2007; 11:564–570. [PubMed: 17920318]
9. Ghasia FF, El-Dairi M, Freedman SF, Rajani A, Asrani S. Reproducibility of Spectral-Domain Optical Coherence Tomography Measurements in Adult and Pediatric Glaucoma. J Glaucoma. 201310.1097/IJG.0b013e31829521db
10. Ghasia FF, Freedman SF, Rajani A, Holgado S, Asrani S, El-Dairi M. Optical coherence tomography in paediatric glaucoma: time domain versus spectral domain. Brit J Ophthalmol. 2013; 97:837–842. [PubMed: 23620420]
11. Hess DB, Asrani SG, Bhide MG, Enyedi LB, Stinnett SS, Freedman SF. Macular and retinal nerve fiber layer analysis of normal and glaucomatous eyes in children using optical coherence tomography. Am J Ophthalmol. 2005; 139:509–517. [PubMed: 15767062]
12. Tariq YM, Pai A, Li H, et al. Association of birth parameters with OCT measured macular and retinal nerve fiber layer thickness. Invest Ophthalmol Vis Sci. 2011; 52:1709–1715. [PubMed: 21212177]
13. Akerblom H, Holmstrom G, Eriksson U, Larsson E. Retinal nerve fibre layer thickness in school-aged prematurely-born children compared to children born at term. Brit J Ophthalmol. 2012; 96:956–960. [PubMed: 22569283]
14. Wang J, Spencer R, Leffler JN, Birch EE. Characteristics of peripapillary retinal nerve fiber layer in preterm children. Am J Ophthalmol. 2012; 153:850–855. [PubMed: 22310079]
15. Wang XY, Huynh SC, Rochtchina E, Mitchell P. Influence of birth parameters on peripapillary nerve fiber layer and macular thickness in six-year-old children. Am J Ophthalmol. 2006; 142:505–507. [PubMed: 16935605]
16. Salchow DJ, Oleynikov YS, Chiang MF, et al. Retinal nerve fiber layer thickness in normal children measured with optical coherence tomography. Ophthalmology. 2006; 113:786–791. [PubMed: 16650674]
17. Huynh SC, Wang XY, Rochtchina E, Mitchell P. Peripapillary retinal nerve fiber layer thickness in a population of 6-year-old children: findings by optical coherence tomography. Ophthalmology. 2006; 113:1583–1592. [PubMed: 16949443]
18. El-Dairi MA, Asrani SG, Enyedi LB, Freedman SF. Optical coherence tomography in the eyes of normal children. Arch Ophthalmol. 2009; 127:50–58. [PubMed: 19139338]
19. Turk A, Ceylan OM, Arici C, et al. Evaluation of the nerve fiber layer and macula in the eyes of healthy children using spectral-domain optical coherence tomography. Am J Ophthalmol. 2012; 153:552–559. [PubMed: 22019223]
20. Tsai DC, Huang N, Hwu JJ, Jueng RN, Chou P. Estimating retinal nerve fiber layer thickness in normal schoolchildren with spectral-domain optical coherence tomography. Jpn J Ophthalmol. 2012; 56:362–370. [PubMed: 22618665]
21. Elia N, Pueyo V, Altemir I, Oros D, Pablo LE. Normal reference ranges of optical coherence tomography parameters in childhood. Brit J Ophthalmol. 2012; 96:665–670. [PubMed: 22328811]
22. Yanni SE, Wang J, Cheng CS, et al. Normative reference ranges for the retinal nerve fiber layer, macula, and retinal layer thicknesses in children. Am J Ophthalmol. 2013; 155:354–360. [PubMed: 23127751]
23. Ozkasap S, Turkyilmaz K, Dereci S, et al. Assessment of peripapillary retinal nerve fiber layer thickness in children with vitamin B12 deficiency. Childs Nerv Syst. 2013; 29:2281–2286. [PubMed: 23677174]
24. Pawar N, Maheshwari D, Ravindran M, Ramakrishnan R. Retinal nerve fiber layer thickness in normal Indian pediatric population measured with optical coherence tomography. Indian J Ophthalmol. 2014; 62:412–418. [PubMed: 24817744]
25. Provis JM, van Driel D, Billson FA, Russell P. Human fetal optic nerve: overproduction and elimination of retinal axons during development. J Comp Neurol. 1985; 238:92–100. [PubMed: 4044906]
26. Dolman CL, McCormick AQ, Drance SM. Aging of the optic nerve. Arch Ophthalmol. 1980; 98:2053–2058. [PubMed: 7436843]

27. Rimmer S, Keating C, Chou T, et al. Growth of the human optic disk and nerve during gestation, childhood, and early adulthood. Am J Ophthalmol. 1993; 116:748–753. [PubMed: 8250079]
28. Scott AW, Farsiu S, Enyedi LB, Wallace DK, Toth CA. Imaging the infant retina with a hand-held spectral-domain optical coherence tomography device. Am J Ophthalmol. 2009; 147:364–373. [PubMed: 18848317]
29. Maldonado RS, Izatt JA, Sarin N, et al. Optimizing hand-held spectral domain optical coherence tomography imaging for neonates, infants, and children. Invest Ophthalmol Vis Sci. 2010; 51:2678–2685. [PubMed: 20071674]
30. Lee AC, Maldonado RS, Sarin N, et al. Macular features from spectral-domain optical coherence tomography as an adjunct to indirect ophthalmoscopy in retinopathy of prematurity. Retina. 2011; 31:1470–1482. [PubMed: 21792089]
31. Chavala SH, Farsiu S, Maldonado R, Wallace DK, Freedman SF, Toth CA. Insights into advanced retinopathy of prematurity using handheld spectral domain optical coherence tomography imaging. Ophthalmology. 2009; 116:2448–2456. [PubMed: 19766317]
32. Allingham MJ, Cabrera MT, O'Connell RV, et al. Racial variation in optic nerve head parameters quantified in healthy newborns by handheld spectral domain optical coherence tomography. J AAPOS. 2013; 17:501–506. [PubMed: 24160971]
33. Tong AY, El-Dairi M, Maldonado RS, et al. Evaluation of optic nerve development in preterm and term infants using handheld spectral-domain optical coherence tomography. Ophthalmology. 2014; 121:1818–1826. [PubMed: 24811961]
34. Moreno TA, O'Connell RV, Chiu SJ, et al. Choroid development and feasibility of choroidal imaging in the preterm and term infants utilizing SD-OCT. Invest Ophthalmol Vis Sci. 2013; 54:4140–4147. [PubMed: 23652488]
35. Maldonado RS, O'Connell R, Ascher SB, et al. Spectral-domain optical coherence tomographic assessment of severity of cystoid macular edema in retinopathy of prematurity. Arch Ophthalmol. 2012; 130:569–578. [PubMed: 22232366]
36. Maldonado RS, O'Connell RV, Sarin N, et al. Dynamics of human foveal development after premature birth. Ophthalmology. 2011; 118:2315–2325. [PubMed: 21940051]
37. Hendrickson A, Possin D, Vajzovic L, Toth CA. Histologic development of the human fovea from midgestation to maturity. Am J Ophthalmol. 2012; 154:767–778. [PubMed: 22935600]
38. Vajzovic L, Hendrickson AE, O'Connell RV, et al. Maturation of the human fovea: correlation of spectral-domain optical coherence tomography findings with histology. Am J Ophthalmol. 2012; 154:779–789. [PubMed: 22898189]
39. Maldonado RS, Yuan E, Tran-Viet D, et al. Three-dimensional assessment of vascular and perivascular characteristics in subjects with retinopathy of prematurity. Ophthalmology. 2014; 121:1289–1296. [PubMed: 24461542]
40. Rothman AL, Tran-Viet D, Gustafson KE, et al. Poorer Neurodevelopmental Outcomes Associated with Cystoid Macular Edema Identified in Preterm Infants in the Intensive Care Nursery. Ophthalmology. 201410.1016/j.ophtha.2014.09.022
41. Avery RA, Cnaan A, Schuman JS, et al. Reproducibility of Circumpapillary Retinal Nerve Fiber Layer Measurements Using Handheld Optical Coherence Tomography in Sedated Children. Am J Ophthalmol. 201410.1016/j.ajo.2014.06.017
42. Altemir I, Pueyo V, Elia N, Polo V, Larrosa JM, Oros D. Reproducibility of optical coherence tomography measurements in children. Am J Ophthalmol. 2013; 155:171–176. [PubMed: 22967864]
43. Prakalapakorn SG, Freedman SF, Lokhnygina Y, et al. Longitudinal reproducibility of optical coherence tomography measurements in children. J AAPOS. 2012; 16:523–528. [PubMed: 23237748]
44. Cabrera MT, Maldonado RS, Toth CA, et al. Subfoveal fluid in healthy full-term newborns observed by handheld spectral-domain optical coherence tomography. Am J Ophthalmol. 2012; 153:167–175. [PubMed: 21925640]
45. He L, Ren R, Yang H, et al. Anatomic vs. acquired image frame discordance in spectral domain optical coherence tomography minimum rim measurements. PLoS One. 201410.1371/journal.pone.0092225

46. Chauhan BC, Burgoyne CF. From clinical examination of the optic disc to clinical assessment of the optic nerve head: a paradigm change. Am J Ophthalmol. 2013; 156:218–227. [PubMed: 23768651]
47. Chiu SJ, Li XT, Nicholas P, Toth CA, Izatt JA, Farsiu S. Automatic segmentation of seven retinal layers in SDOCT images congruent with expert manual segmentation. Opt Express. 2010; 18:19413–194128. [PubMed: 20940837]
48. Schuman JS, Pedut-Kloizman T, Hertzmark E, et al. Reproducibility of nerve fiber layer thickness measurements using optical coherence tomography. Ophthalmology. 1996; 103:1889–1898. [PubMed: 8942887]
49. De Silva DJ, Cocker KD, Lau G, Clay ST, Fielder AR, Moseley MJ. Optic disk size and optic disk-to-fovea distance in preterm and full-term infants. Invest Ophthalmol Vis Sci. 2006; 47:4683–4686. [PubMed: 17065474]
50. Williams TD, Wilkinson JM. Position of the fovea centralis with respect to the optic nerve head. Optometry Vision Sci. 1992; 69:369–377.
51. Cohen MJ, Kaliner E, Frenkel S, Kogan M, Miron H, Blumenthal EZ. Morphometric analysis of human peripapillary retinal nerve fiber layer thickness. Invest Ophthalmol Vis Sci. 2008; 49:941–944. [PubMed: 18326716]
52. Gordon RA, Donzis PB. Refractive development of the human eye. Arch Ophthalmol. 1985; 103:785–789. [PubMed: 4004614]
53. Oner V, Ozgur G, Turkyilmaz K, Sekeryapan B, Durmus M. Effect of axial length on retinal nerve fiber layer thickness in children. Eur J Ophthalmol. 2014; 24:265–272. [PubMed: 23918073]
54. Aykut V, Oner V, Tas M, Iscan Y, Agachan A. Influence of axial length on peripapillary retinal nerve fiber layer thickness in children: a study by RTVue spectral-domain optical coherence tomography. Curr Eye Res. 2013; 38:1241–1247. [PubMed: 23972028]

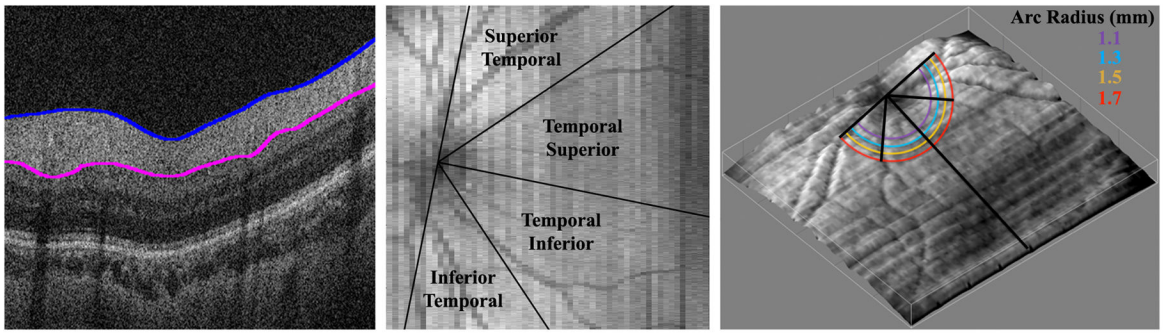

Figure 1. Retinal Nerve Fiber Layer Segmentation and Average Sectoral Thickness Measurements

Left, Spectral domain optical coherence tomography (SDOCT) B-scan cross-sectional image from the macula of a healthy Hispanic male born and imaged at 39 weeks post-menstrual age. Inner (blue) and outer (pink) boundaries of the retinal nerve fiber layer (RNFL) are segmented, or outlined, utilizing a custom MATLAB script (Mathworks, Inc., Natick, MA). **Middle,** summed voxel projection derived from SDOCT scan of the same full-term infant. Temporal retina is divided into four 45° sectors, considered, from superior to inferior, the superior temporal, temporal superior, temporal inferior, and inferior temporal retina. Mean RNFL thicknesses can be calculated over each sector of segmented SDOCT scan. Note that the temporal superior and temporal inferior sectors may be assessed together as the 90° temporal quadrant. **Right,** three-dimensional retinal surface rendering map of the same healthy, full-term infant derived from SDOCT scan using ImageJ (National Institute of Health, Bethesda, MD). The organizing axis originates from the center of the optic nerve and travels through the fovea. The mean RNFL thickness was measured at distances of 1.1, 1.3, 1.5, and 1.7 mm from the center of the optic nerve, represented by the concentric color arcs.

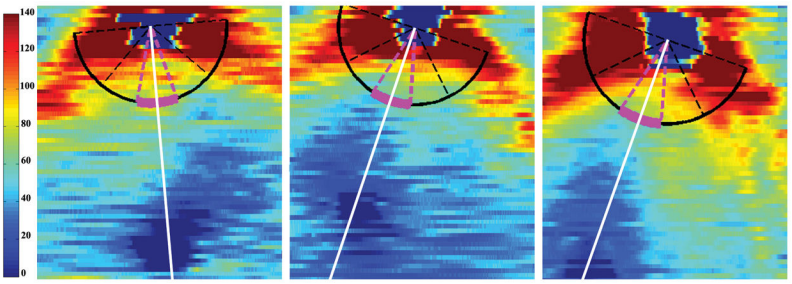

Figure 2. Retinal Nerve Layer Thickness Maps

Retinal nerve fiber layer (RNFL) thickness maps derived from segmented spectral domain optical coherence tomography scans of three full-term, healthy infants. The organizing axis originates from the center of the optic nerve and travels through the fovea. The magenta arc denotes the papillomacular bundle, defined as the 30° arc from −15° to +15° on the axis from the optic nerve to fovea and also referred to as the 9 o'clock hour for right eyes and 3 o'clock hour for left eyes. **Left,** RNFL thickness map of a Black female born and imaged at 40 weeks post-menstrual age. **Middle,** RNFL thickness map of a White male born and imaged at 40 weeks post-menstrual age. **Right,** RNFL thickness map of a Hispanic female born and imaged at 38 weeks post-menstrual age.

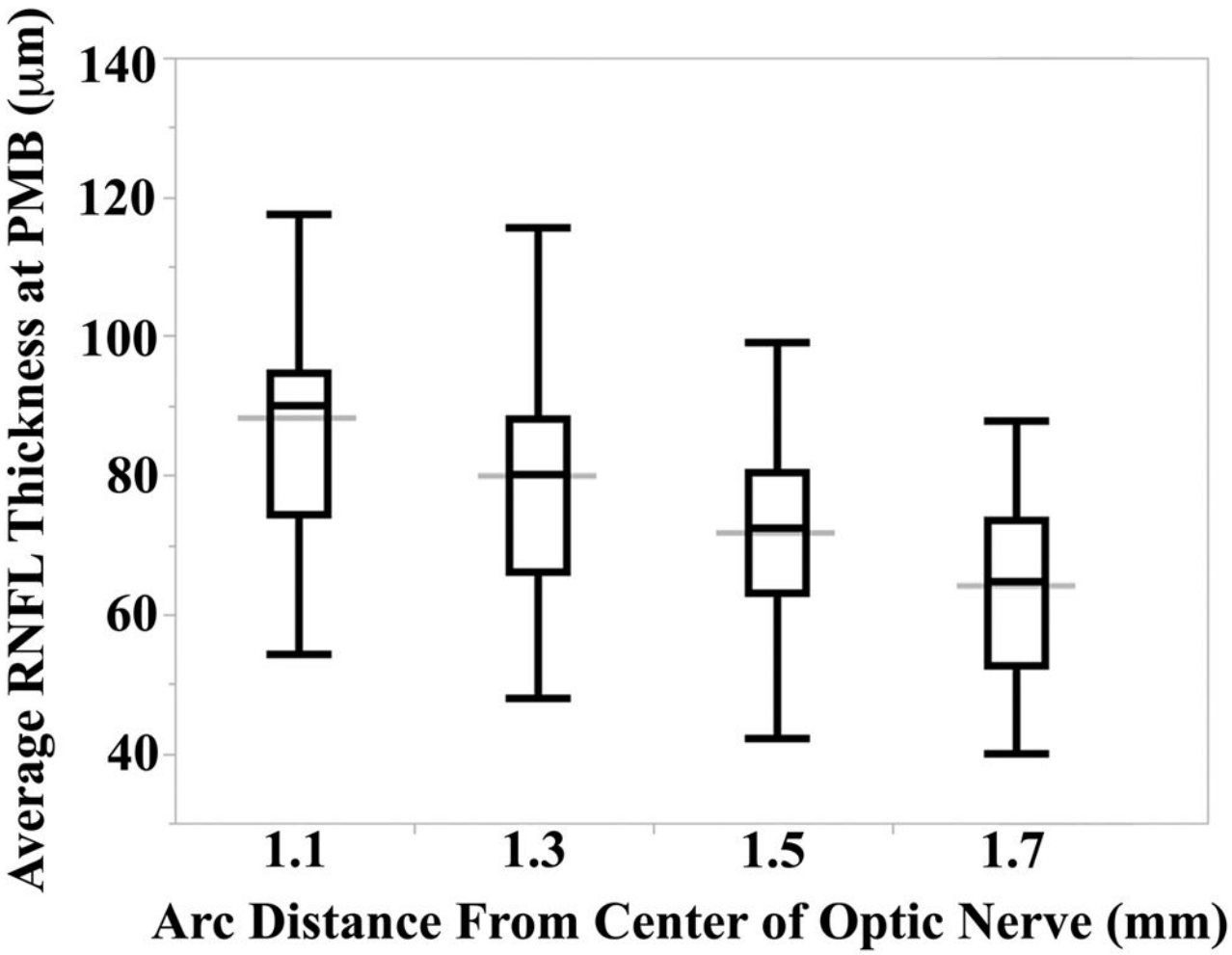

Figure 3. Average Retinal Nerve Fiber Layer Thickness Varies by Radial Distance from the Optic Nerve

Distributions of the average retinal nerve fiber layer thicknesses (RNFL) by arc distance from the center of the optic nerve. All arcs were measured along the papillomacular bundle (PMB), defined as the 30° arc from −15° to +15° on the axis from the optic nerve through the fovea. Note that the distributions at 1.1 and 1.3 mm distance contain 49 full-term infants while the distributions at 1.5 and 1.7 mm distance contain all 50 full-term infants. The black box and whisker plots represent the minimum, 25%, median, 75%, and maximum RNFL thickness measured at each distance. The wider gray line represents the overall mean RNFL for each distance along the PMB. The Shapiro-Wilk W test of normality P-values at 1.1, 1.3, 1.5, and 1.7 mm radial distances were 0.11, 0.22, 0.60, and 0.34, respectively. Analysis of variance demonstrated an inverse relationship between average RNFL thickness along the PMB and radial distance from the center of the optic nerve ($P<0.001$).

Table 1

Mean Retinal Nerve Fiber Layer Sector Thicknesses by Race in Full-Term, Healthy Infants

	Superior Temporal			Temporal Superior			Temporal Inferior			Inferior Temporal			Temporal		
	n	RNFL, µm Mean (SD)	P-Value*	n	RNFL, µm Mean (SD)	P-Value*	n	RNFL, µm Mean (SD)	P-Value*	n	RNFL, µm Mean (SD)	P-Value*	n	RNFL, µm Mean (SD)	P-Value*
Race			0.04			0.41			0.24			0.28			0.26
Black	10	128 (27)		12	79 (18)		12	90 (20)		9	124 (16)		12	85 (16)	
Hispanic	18	124 (30)		19	85 (22)		19	87 (22)		16	123 (33)		19	86 (16)	
White	13	100 (19)		17	78 (19)		18	79 (19)		15	109 (30)		17	79 (14)	

RNFL, retinal nerve fiber layer; SD, standard deviation

*P-Value calculated by Kruskal-Wallis test.

Note that with Bonferroni correction, a significant difference is detected between groups for P<0.01

Table 2

Pediatric Retinal Nerve Fiber Layer Thickness Measurements in the Literature

Study	Year	N	OCT Device	Radial Distance mm	Age at Imaging, Mean (SD), yr	Temporal Mean (SD), μm	Superior Temporal Mean (SD), μm	Inferior Temporal Mean (SD), μm
Rothman et al.	2014	50	HH Bioptigen[a]	1.5	39.2 (1.1)[b]	83 (16)	115 (28)	118 (29)
				1.7		74 (15)	103 (26)	105 (28)
Hess et al.[11]	2005	36	Stratus OCT-3[c]	1.7	9.5 (3.5)	---	129.5 (21.8)	133.4 (23.2)
Salchow et al.[16]	2006	92	Stratus OCT-3[c]	1.7	9.7 (2.7)	72.5 (13.4)	---	---
Huynh et al.[17]	2006	1369	Stratus OCT-3[c]	1.73	6.7 (0.4)	75.7 (14.7)	---	---
El-Dairi et al.[18]	2009	286	Stratus OCT-3[c]	1.73	8.6 (3.1)	78 (56–105)[d]	---	---
Turk et al.[19]	2012	107	Spectralis[e]	1.75	10.5 (2.9)	74.3 (9.4)	139.0 (17.6)	144.6 (17.2)
Tsai et al.[20]	2012	265	RTVue-100[f]	1.73	7.1 (6.5–7.9)[g]	87.8 (86.2–89.3)[d]	---	---
Elia et al.[21]	2012	357	Cirrus[c]	1.73	9.2 (1.7)	69.4 (11.3)	---	---
Akerblom et al.[13]	2012	54	Stratus OCT-3[c]	1.7	10.2 (3.1)	69 (58–83)[g]	---	---
Yanni et al.[22]	2013	83	Spectralis[e]	1.75	9.1 (2.5)	76.5 (1.9)	145.1 (2.2)	147.0 (2.1)
Ozkasap et al.[23]	2013	66	Cirrus[c]	1.73	13.4 (2.4)	66.6 (9.6)	---	---
Avery et al.[5]	2014	31	HH Bioptigen[a]	1.73	8.7 (1.7–16.7)[h]	105.5 (14.0)	---	---
Pawar et al.[24]	2014	120	Stratus OCT-3[c]	1.73	10.8 (3.2)	70.7 (14.8)	---	---

OCT, optical coherence tomography; SD, standard deviation, HH, handheld

[a] Bioptigen, Inc., Research Triangle Park, NC

[b] weeks post-menstrual age

[c] Carl Zeiss Meditec, Inc., Dublin, CA

[d] mean (5^{th} percentile – 95^{th} percentile)

[e] Heidelberg Engineering, Inc., Carlsbad, CA

[f] Optovue Inc., Fremont, CA

[g] mean (range)

[h] median (range)